ADVANCED MATERIALS
www.advmat.de

MXenes for Plasmonic Photodetection

*Dhinesh Babu Velusamy, Jehad K. El-Demellawi, Ahmed M. El-Zohry, Andrea Giugni, Sergei Lopatin, Mohamed N. Hedhili, Ahmed E. Mansour, Enzo Di Fabrizio, Omar F. Mohammed, and Husam N. Alshareef**

Dr. D. B. Velusamy, J. K. El-Demellawi, Dr. A. M. El-Zohry, Dr. A. Giugni, Dr. A. E. Mansour, Prof. E. Di Fabrizio, Prof. O. F. Mohammed, Prof. H. N. Alshareef
Physical Science and Engineering Division
King Abdullah University of Science and Technology (KAUST), Thuwal 23955-6900, Kingdom of Saudi Arabia

DOI: 10.1002/adma.201807658

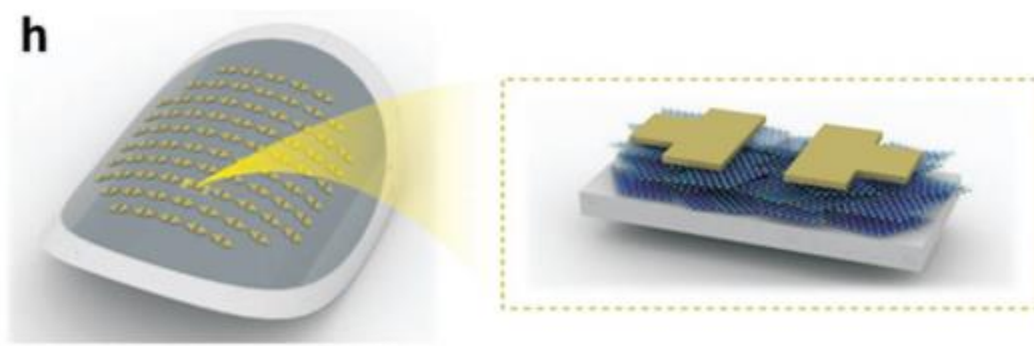

Sandeep Bose
6-7-19

MXenes

MXenes, discovered in 2011, are ceramics that comprise one of the largest families of two-dimensional (2D) materials. MXenes are made from a bulk crystal called MAX. Unlike most 2D ceramics, MXenes have inherently good conductivity because they are molecular sheets made from the carbides and nitrides of transition metals.

Example: Ti_2C, $(Ti_{0.5},Nb_{0.5})_2C$, V_2C, Nb_2C, Mo_2C, Ti_3C_2, Ti_3CN, Zr_3C_2, Hf_3C_2, Ti_4N_3, Nb_4C_3 , Ta_4C_3, Mo_2TiC_2, Cr_2TiC_2, $Mo_2Ti_2C_3$

Applications:

- Water purification and desalination
- Energy storage
- Triboelectric nanogenerator
- Conductive coating
- Sensors

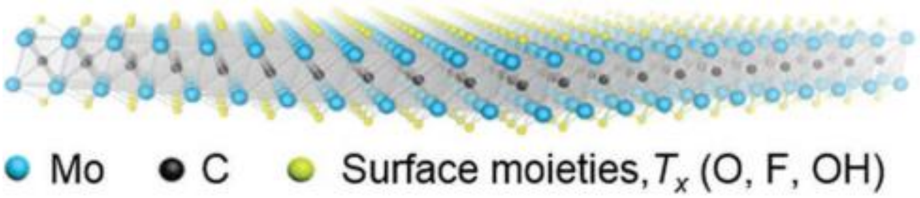

Relevance to the group

1. Water purification/Desalination

The Journal of Physical Chemistry Letters

ACS AuthorChoice

Letter

pubs.acs.org/JPCL

Charge- and Size-Selective Ion Sieving Through $Ti_3C_2T_x$ MXene Membranes

Chang E. Ren,[†] Kelsey B. Hatzell,[†] Mohamed Alhabeb,[†] Zheng Ling,[†] Khaled A. Mahmoud,[*,‡] and Yury Gogotsi[*,†]

[†]Department of Materials Science and Engineering and A. J. Drexel Nanomaterials Institute, Drexel University, Philadelphia, Pennsylvania 19104, United States

[‡]Qatar Environment and Energy Research Institute, P.O. Box 5825, Doha, Qatar

ABSTRACT: Nanometer-thin sheets of 2D $Ti_3C_2T_x$ (MXene) have been assembled into freestanding or supported membranes for the charge- and size-selective rejection of ions and molecules. MXene membranes with controllable thicknesses ranging from hundreds of nanometers to several micrometers exhibited flexibility, high mechanical strength, hydrophilic surfaces, and electrical conductivity that render them promising for separation applications. Micrometer-thick MXene membranes demonstrated ultrafast water flux of 37.4 L/(Bar·h·m^2) and differential sieving of salts depending on both the hydration radius and charge of the ions. Cations with a larger charge and hydration radii smaller than the interlayer spacing of MXene (~6 Å) demonstrate an order of magnitude slower permeation compared to single-charged cations. Our findings may open a door for developing efficient and highly selective separation membranes from 2D carbides.

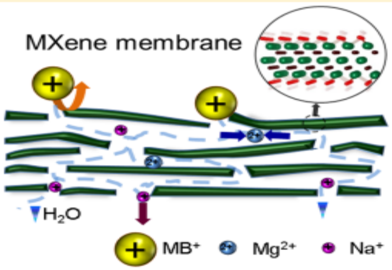

2. Energy storage

ADVANCED MATERIALS
www.advmat.de

Materials Views
www.MaterialsViews.com

Two-Dimensional Nanocrystals Produced by Exfoliation of Ti_3AlC_2

Michael Naguib, Murat Kurtoglu, Volker Presser, Jun Lu, Junjie Niu, Min Heon, Lars Hultman, Yury Gogotsi, and Michel W. Barsoum**

Adv. Mater. **2011**, *23*, 4248–4253

3. Triboelectric nanogenerator

Contents lists available at ScienceDirect

Nano Energy

journal homepage: www.elsevier.com/locate/nanoen

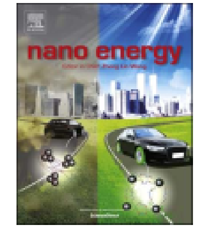

Full paper

Metallic MXenes: A new family of materials for flexible triboelectric nanogenerators

Yongchang Dong[a,1], Sai Sunil Kumar Mallineni[a,1], Kathleen Maleski[c], Herbert Behlow[a], Vadym N. Mochalin[b], Apparao M. Rao[a], Yury Gogotsi[c,*], Ramakrishna Podila[a,**]

[a] *Department of Physics and Astronomy, Clemson Nanomaterials Institute, Clemson University, Clemson, SC 29634, USA*
[b] *Department of Chemistry and Department of Materials Science & Engineering, Missouri University of Science & Technology, Rolla, MO 65409, USA*
[c] *A.J. Drexel Nanomaterials Institute, and Department of Materials Science and Engineering, Drexel University, Philadelphia, PA 19104, USA*

Nano Energy 44 (2018) 103–110

What’s new

Detail investigation of plasmonic properties associated with their ultrathin-atomic-layer structure and their potential use in photonic and plasmonic devices has been explored here.

Introduction

- MXenes, a thriving family of transition metal-based 2D materials, have garnered signifcant interest due to their intriguing physicochemical properties and solution processability.

- Thus far, owing to their promising electrochemical characteristics, this new class of 2D materials has been predominantly used in energy conversion and storage applications.

- MXenes have recently exhibited impressive optical properties e.g., tunable broadband absorption and intense surface plasmon excitations, underlining their potential for optoelectronic and plasmonic applications. However, theoretical and experimental investigations in this context remain sparse and mainly limited to the most studied Ti3C2T*x* MXene.

- In this work, five different Mxene nanosheets, i.e., Mo2CT*x*, Ti3C2T*x*, Nb2CT*x*,T2CT*x*, and V2CT*x*, were first synthesized from their parent MAX phase and their structural, morphological, and steady state optical characteristics were studied.

- Among the five studied MXenes, Mo2CT*x* was selected as a model system for its relative stability against oxidation, moderately high free carrier density, and electrical conductivity, mechanical flexibility, good responsivity and detectivity.

- For the first time, Mo2CT*x* thin film photodetectors was deomonstrated that operate in the visible spectral region. It is worth mentioning that the responsivity of the Mo2CT*x* Mxene devices is ≈18 000 and ≈1200 times higher than the first reported graphene and Mos2 photoconductors.

Synthesis

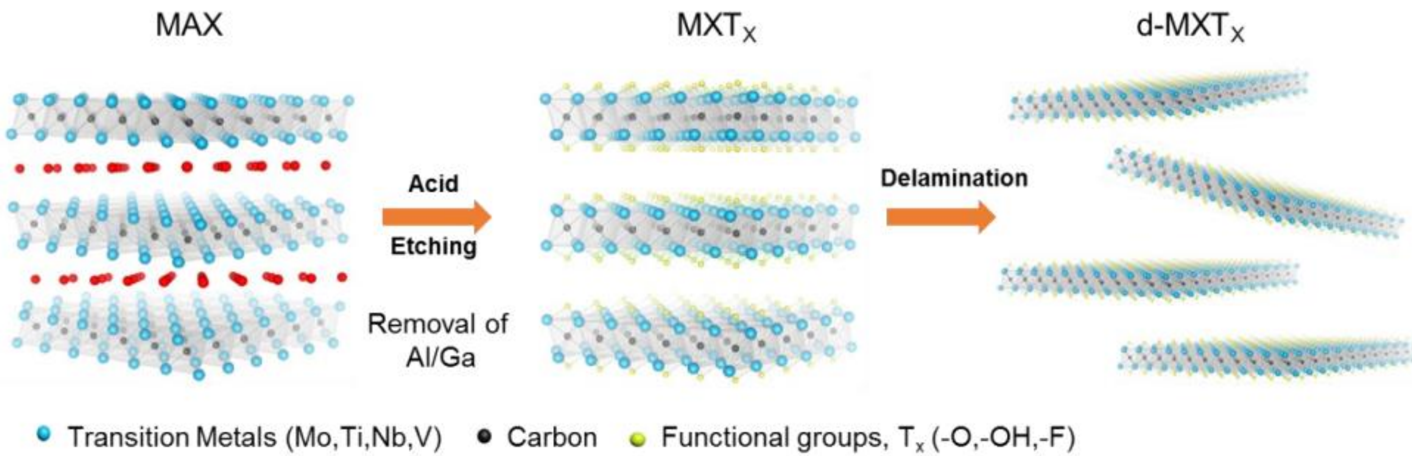

- To synthesize Mo2C*Tx*, 2g of Mo2Ga2C MAX powder was immersed into 20 ml of 47-51% HF.

- The mixtures were then stirred with a magnetic Teflon stir bar at room temperature for168 h.

- Following the HF treatment, the acidic suspensions of Mo2C*Tx* were washed using cold deionized water. After discarding the supernatant solution, the solid sediment was kept under vacuum overnight for drying at room temperature.

- Dried multilayer Mo2C*Tx* Mxene powder was further re-dispersed into 10 ml of 54-56% tetrabutylammonium hydroxide solution for intercalation, and stirred for 4 h at room temperature.

- The resulting mixtures were washed three times, and sediments were re-dispersed into cold deionized water followed by ultra-sonication for an hour. The mixtures were later centrifuged the dispersions were used for the thin film fabrication.

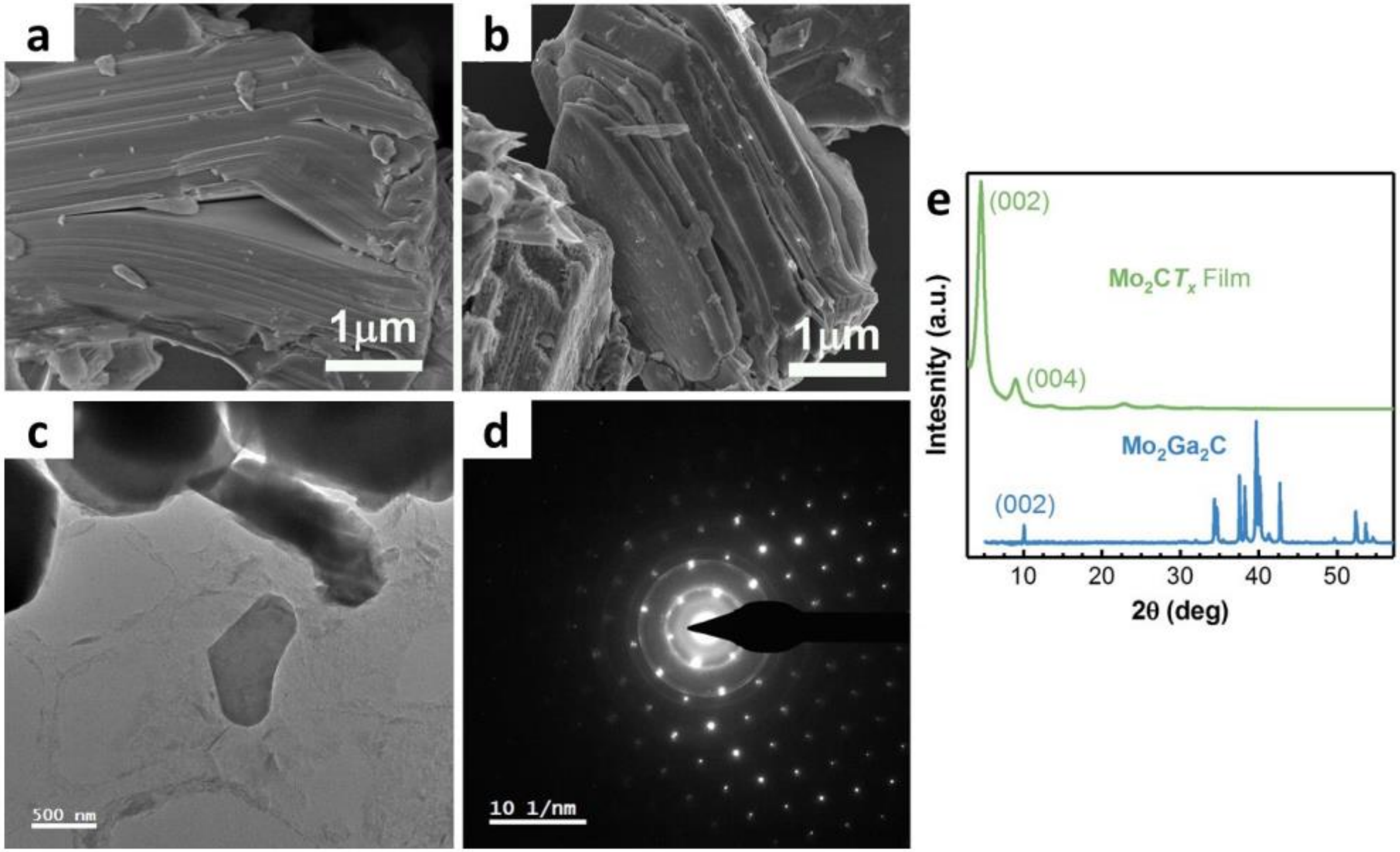

Figure 1. Secondary electron SEM images for **a,** unreacted multilayered Mo2Ga2C MAX and **b,** exfoliated Mo2C*Tx*. **c,** Bright-field TEM image of a representative Mo2C*Tx* nanoheet, and **d,** its corresponding SAED pattern. **e,** XRD patterns of Mo2Ga2C MAX (blue) and the corresponding intercalated-Mo2C*Tx* MXene film (green).

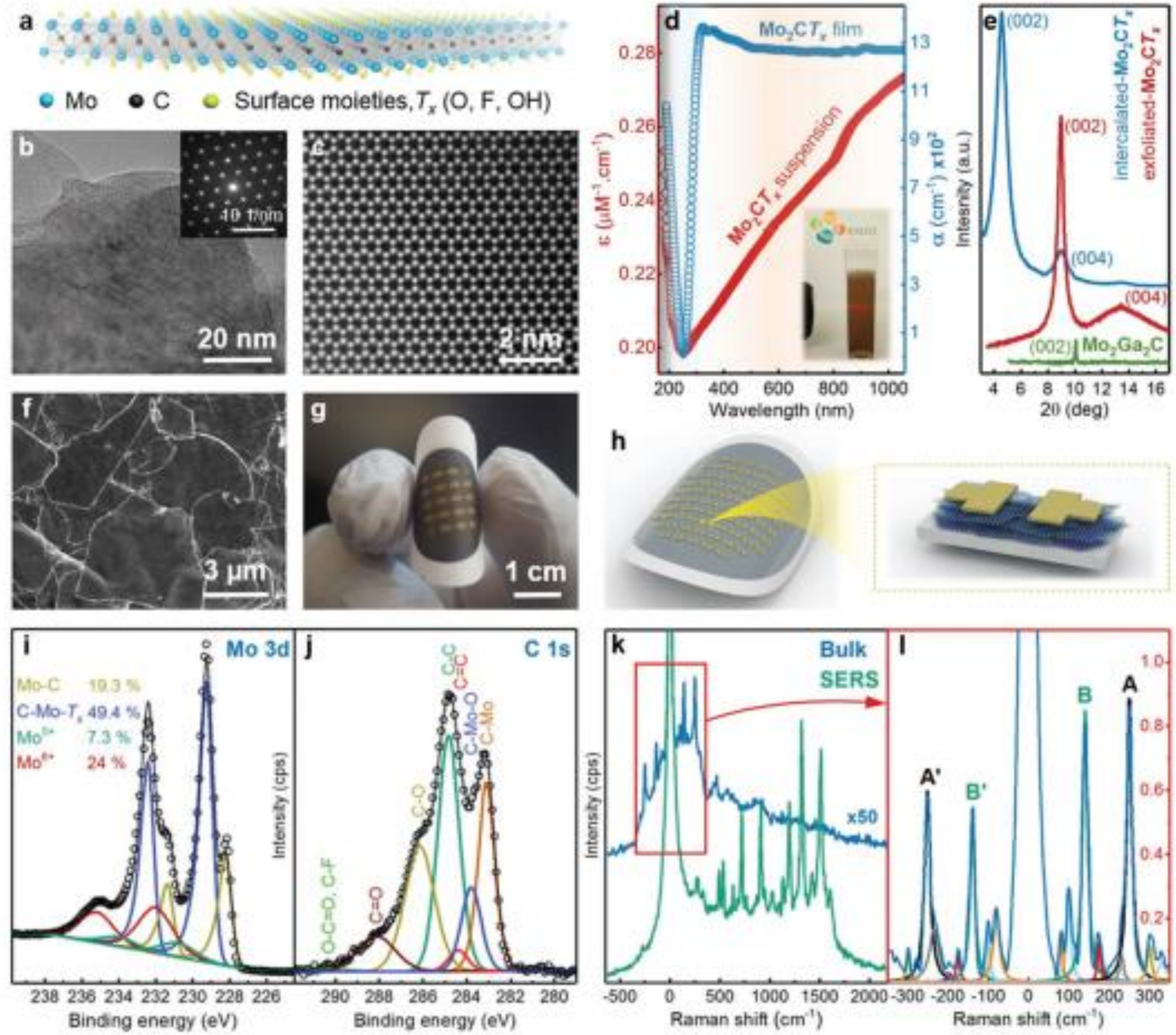

Figure 2. a) Schematic illustration of a delaminated Mo2CT*x* nanosheet b) TEM image of few-layered Mo2CT*x* nanosheets. Inset: Fast Fourier transform (FFT) pattern. c) High-resolution STEM Image of Mo2CT*x*. d) UV–vis–NIR absorption spectra of Mo2CT*x* film (blue, 1.8 µm) and dispersed in water (red, 0.6 mg mL-1) with a minimum at ≈250 nm, representing the onset of free carrier absorption. e) XRD patterns of Mo2Ga2C (green), exfoliated-Mo2CT*x* (red),and intercalated-Mo2CT*x* (blue) at low Bragg's angles.f) SEM micrograph showing the surface morphology of a Mo2CT*x* thin film. g) Photograph and h) schematic illustration of an array of two terminal, parallel-type thin flm Mo2CT*x* Based flexible photodetectors. i) High-resolution XPS spectrum of the Mo 3d and j) C 1s core levels. k) Micro-Raman spectroscopy of Mo2CT*x* at 633 nm. (Blue) Resonant Raman scattering spectrum of Mo2CT*x* (Bulk,obtained by averaging more than 1000 spectra). (Green) A surface-enhanced Raman scattering (SERS) spectrum, displayed for comparison, obtained at one position on the Au electrodes. l) Low-frequency range of the Raman spectrum of the bare Mo2CT*x* film. The spectrum is analyzed by Lorentzian functions after subtraction of the broad baseline.

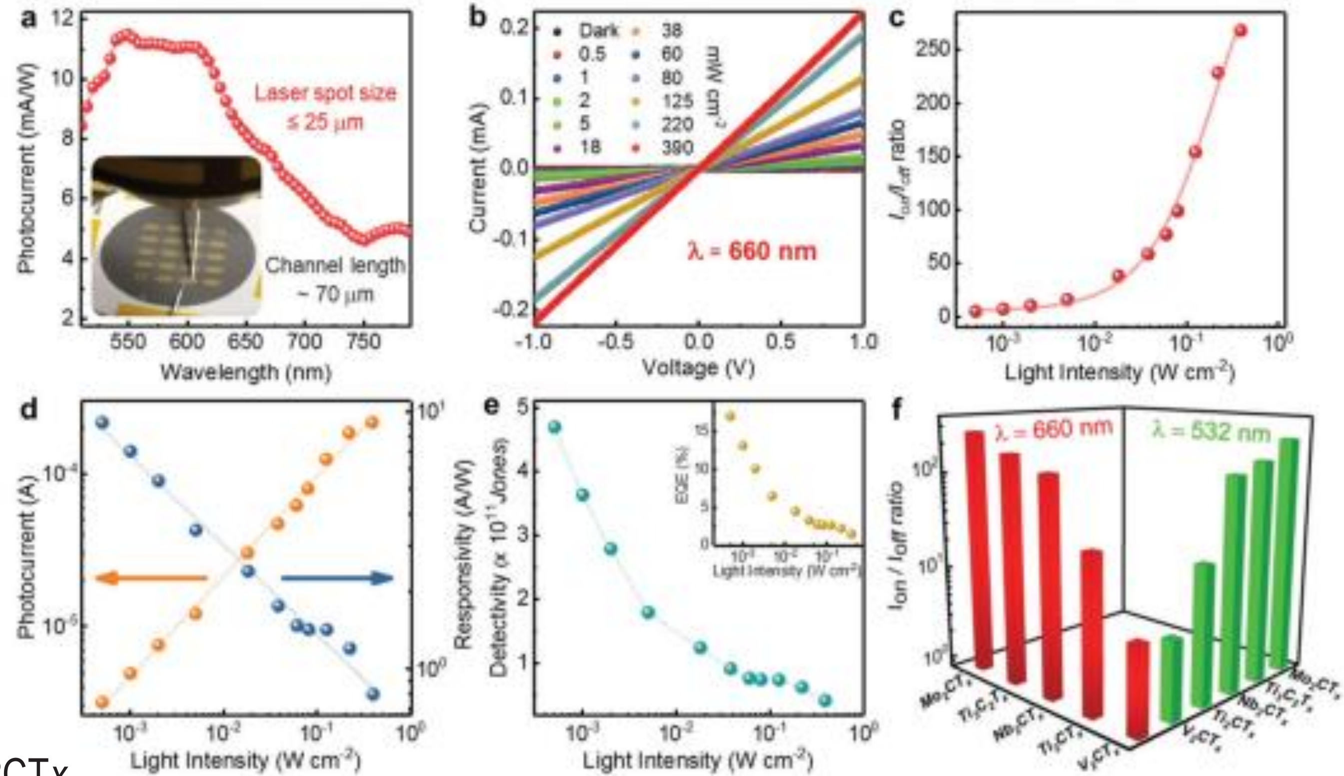

Figure 3. a) Photoresponse of a Mo2CT*x* thin film photodetector as a function of wavelength, under 0.7 V bias voltage Inset: Photograph of the photo current setup showing one of the investigated samples b) Linear scale current–voltage (*I*–*V*) characteristics of the Mo2CT*x* thin flm photodetector in the dark and under different light intensities at a wavelength of 660 nm with a bias voltage of ±1V. c) Ratios of the photocurrent to the dark current of the Mo2CT*x* thin film photo detector as function of different light intensities. d) (Left) Photocurrents of the Mo2CT*x* thin film photodetector as a function of different light intensities with respect to the dark state of the device. (Right) Responsivity of the photodetector as a function of different light intensities. e) The detectivity and EQE (inset) of the photodetector as a function of different light intensities. f) Ratios of the photocurrent of different MXene photodetectors with respect to the dark current, measured at wavelengths of 660 nm (red bars) and 532 nm (green bars). All the values were obtained at light intensities of 0.39 and 0.41 W cm-2 for wavelengths of 660 and 532 nm, respectively. Results shown in (c–e) are obtained considering an excitation at 660nm.

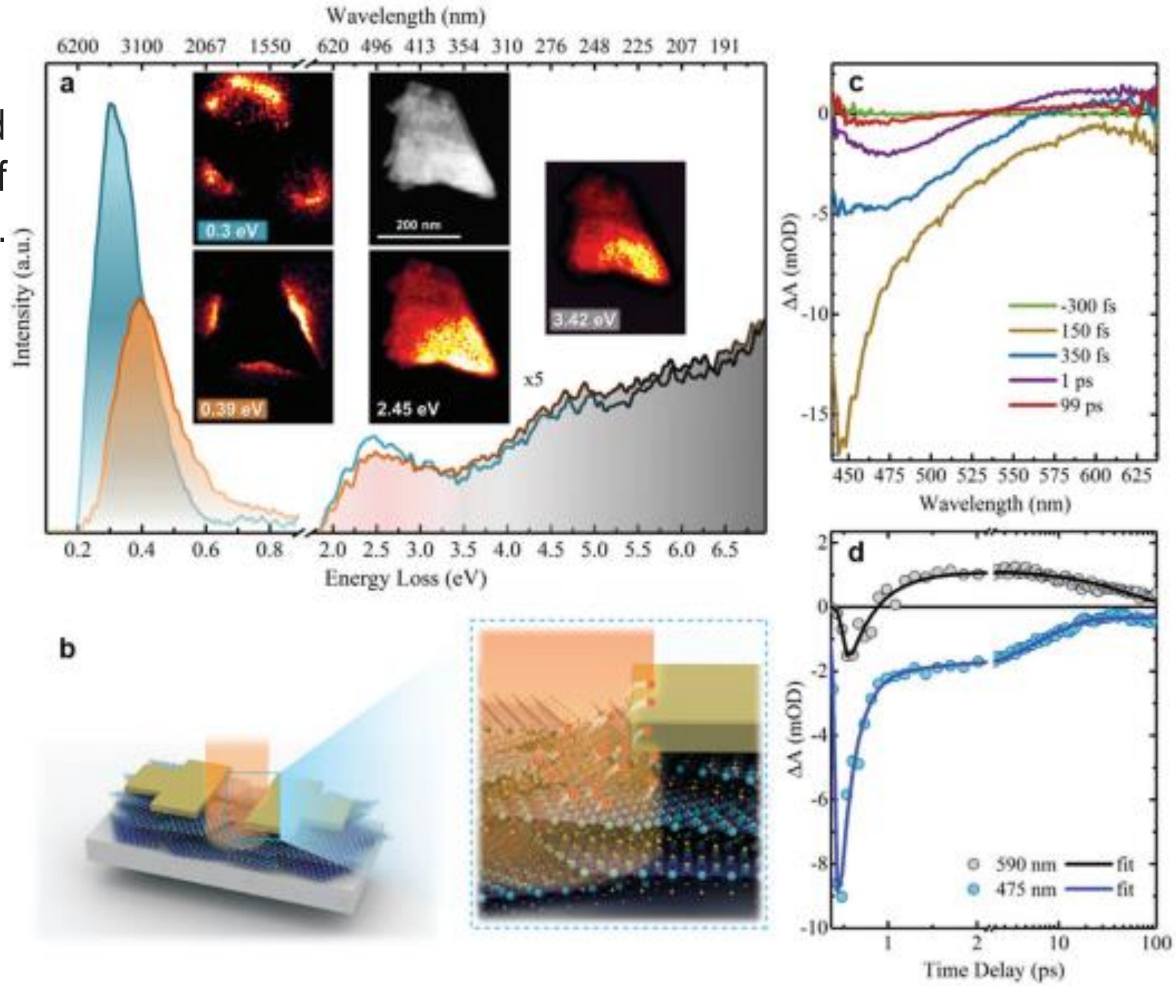

Figure 4. a) ZLPsubtracted EELS acquired on a truncated triangular nanosheet of Mo2CT*x* (≈58 nm ± 1 at the center). The spectra are normalized to the transversal SP peak at 2.45 eV (highlighted in red) and magnified by a factor of 5 above 1.7 eV. Insets: ADF-STEM micrograph of the Mo2CT*x* nanosheet on a Si3N4 supporting membrane (black area), and the EELS fitted intensity maps of the corresponding longitudinal SP modes; namely, dipole (0.3 eV) and quadrupole (0.39 eV), in addition to the transversal SP mode (2.45 eV) and the IBT(starting at 3.42 eV). b) Schematic representation of the photodetector under illumination showing the migration process of the plasmon Assisted hot electrons toward the biased gold electrodes. c) Time-resolved visible transient absorption spectra of Mo2CT*x* at different time slots. d) Kinetic traces of the GSB recovery and ESA decay of Mo2CT*x* extracted at 475 and 590 nm, respectively. These data were collected under excitation wavelength of 330 nm.

Figure 5. a) Photoresponse behavior of Mo2CT*x* thin film photodetector under alternating ON and OFF cycles at a wavelength of 660 nm with a light intensity of 0.22 W cm-2. Both the switch-ON and -OFF times of the detector were ≈500ms. b) Photostability of the Mo2CT*x* thin film photodetectors under continuous illumination of 660 nm light in ambient conditions. The device maintained ≈80% of the initial photocurrent even after ≈12 000 s. c) Ratios of the photocurrent, under 660 nm light illumination, with respect to the dark current as a function of storage time. d) Photocurrent and dark current ratio as a function of the bending radius. e) Ratios of the photocurrent to the dark current of the photodetectors as a function of the number of bending cycles at a bending radius of ≈3 mm. Devices worked properly after 500 bending cycles at a bending radius of ≈3 mm, without any significant deterioration of the performance. All of the values were obtained at a wavelength of 660 nm with a light intensity of 0.22 W cm-2.

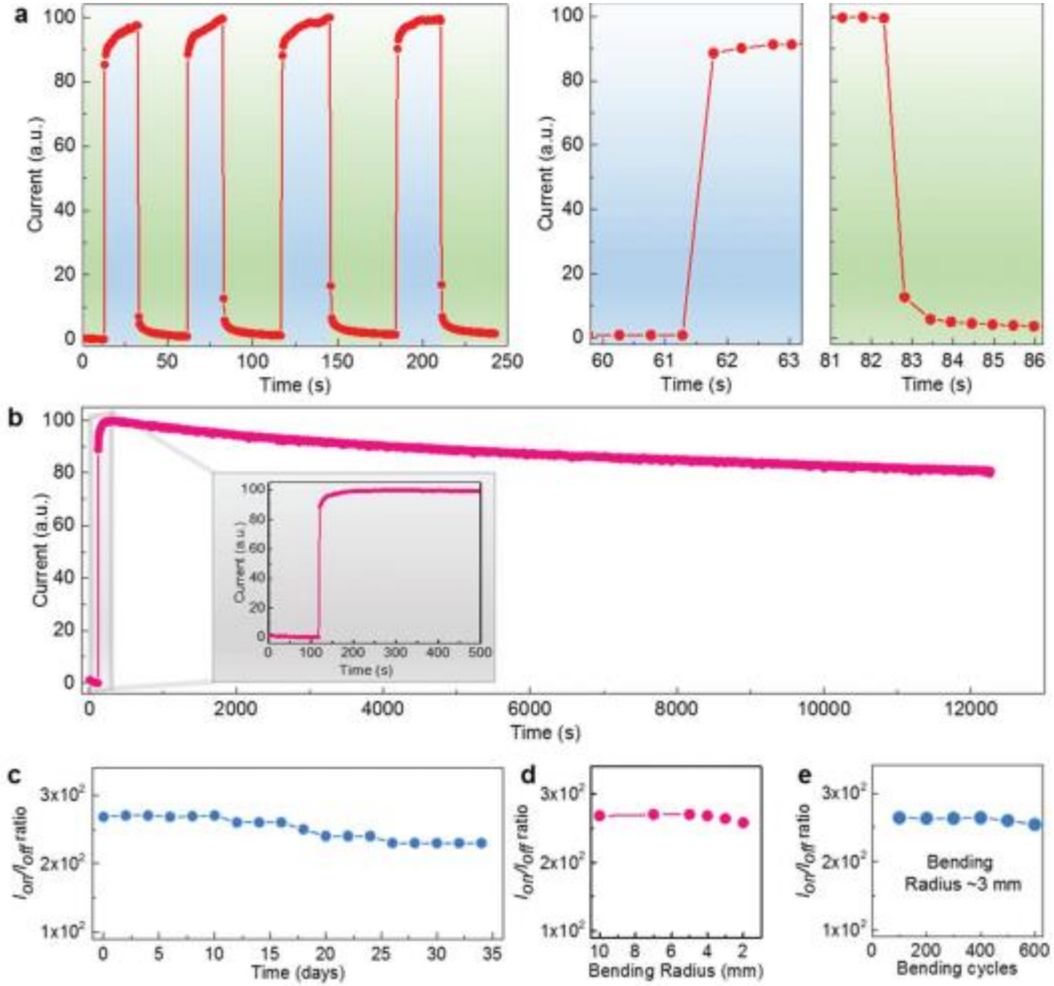

Summary

- In summary, they have fabricated flexible MXene thin film photodetectors operating in the visible spectral region. Their photoresponse is dominated by the intrinsic plasmon-assisted hot carrier generation without the need for integration with other metallic plasmonic structures.
- Despite being the first demonstration of plasmonic photodetection in MXenes, the performance of Mo2CT*x* thin films considering their *R* and *D** is surpassing the majority of previously reported visible-band photodetectors based on solution-processed 2D materials.
- In addition to their attractive performance and solution processability, it was revealed that the MXene-based devices possess additional set of advantages including full visible spectrum coverage, highly stable operation, and mechanical flexibility.
- On the top of that, by means of high-resolution STEM-EELS, they have been able, for the first time, to image the spatial and energy distribution of SP modes over individual Mo2CT*x* nanosheets.
- Further, using the demonstrated ability of coupling with light and dephasing of SPs with a short lifetime have led to a photoresponse outperforming that of photoelectron-based semiconductor devices.
- These findings shed light on the knowledge of photocurrent generation mechanisms in MXenes, making them much more viable for many photonic and plasmonic device applications.